

Accelerating Mobile Audio Sensing Algorithms through On-Chip GPU Offloading

Petko Georgiev[§], Nicholas D. Lane^{†*}, Cecilia Mascolo[§], David Chu[‡]
[§]University of Cambridge, [†]University College London, ^{*}Nokia Bell Labs, [‡]Google

ABSTRACT

GPUs have recently enjoyed increased popularity as general purpose software accelerators in multiple application domains including computer vision and natural language processing. However, there has been little exploration into the performance and energy trade-offs mobile GPUs can deliver for the increasingly popular workload of deep-inference audio sensing tasks, such as, spoken keyword spotting in energy-constrained smartphones and wearables. In this paper, we study these trade-offs and introduce an optimization engine that leverages a series of structural and memory access optimization techniques that allow audio algorithm performance to be automatically tuned as a function of GPU device specifications and model semantics. We find that parameter optimized audio routines obtain inferences an order of magnitude faster than sequential CPU implementations, and up to 6.5x times faster than cloud offloading with good connectivity, while critically consuming 3-4x less energy than the CPU. Under our optimized GPU, conventional wisdom about how to use the cloud and low power chips is broken. Unless the network has a throughput of at least 20Mbps (and a RTT of 25 ms or less), with only about 10 to 20 seconds of buffering audio data for batched execution, the optimized GPU audio sensing apps begin to consume less energy than cloud offloading. Under such conditions we find the optimized GPU can provide energy benefits comparable to low-power reference DSP implementations with some preliminary level of optimization; in addition to the GPU always winning with lower latency.

1. INTRODUCTION

Graphics Processing Units (GPUs) are the method of choice for executing high computational loads and accelerating compute-intensive applications in domains such as computer vision [57, 23, 36] and deep learning [16, 17]. But GPUs like any complex processor architecture need to be used smartly to maximize their throughput and efficiency. There have been extensive studies for graphics and games [57, 36, 57, 50] including mobile [23], but the analysis has largely evaded other general-purpose GPU computations on a mobile device such as audio applications that rely on the power-hungry microphone sensor. Examples of audio sensing apps are personal

digital assistants such as Apple's Siri [2] or Google Now [5], as well as a plethora of behavior monitoring apps that recognize emotions from voice [52, 46], or perform conversation analysis [45, 58, 48]. These applications are capable of deep inferences about user behavior, often require continuous sensor monitoring, and boast highly sophisticated inference algorithms that easily strain scarce mobile resources (battery, memory and computation) [41]. As a result, computational offloading to cloud [24] or low-power co-processors [27, 45] has often been the solution applied to keep these apps functional on the mobile device, but no study has been done on the feasibility of GPU offloading for this data-intensive workload.

In the mobile landscape where energy is the biggest limiting factor, it is not immediately obvious whether accelerating these sensing applications via GPU offloading will result in energy-justified performance boosts compared to the above mentioned alternatives (cloud and low-power co-processors). Questions that we investigate in this paper are: What trade-offs do we get in terms of speed and energy if we express audio sensing algorithms in a GPU-compliant manner? How can we best take advantage of the general-purpose computing capabilities of mobile GPUs to offload audio processing? When should we prefer GPU computation to cloud? Can we obtain energy efficiency on a scale comparable to a low-power Digital Signal Processor (DSP)?

In this work, we show that the GPU performance of audio sensing algorithms is sensitive to two key control-flow parameters such as the frame fan-out (total number of frame processing GPU threads) and per-thread compute factors (amount of computation relative to memory accesses). We present a GPU offloading engine that leverages parallel optimization techniques that allow us to control these parameters and auto-tune the performance of audio routines. Without such optimization, naively parameterized GPU implementations may be up to 1.5x slower than multi-threaded CPU alternatives, and consume more than 2x the energy of cloud offloading.

Through extensive evaluation we find that *for time-sensitive audio apps, and when energy is less of a concern, there is no better option than using GPU optimized audio routines*. Algorithms tuned for the GPU can deliver inferences an order of magnitude faster than a sequential CPU deployment, and 3.1x or 6.5x faster than cloud offloading with good connectivity for deep audio inferences such as speaker identification and keyword spotting, respectively. At the same time, the energy consumed is 3-4x lower than when using the CPU. Perhaps more surprising, *for tasks that are more continuous but tolerate short delays (of 10-20 secs) GPU is also a top choice*. When raw data is accumulated for batched processing, algorithms optimized for the GPU begin to consume less energy than cloud offloading with fast connections. Further, the optimized GPU can deliver energy efficiency levels in ranges comparable to what can be achieved by low-power DSP implementations

Permission to make digital or hard copies of all or part of this work for personal or classroom use is granted without fee provided that copies are not made or distributed for profit or commercial advantage and that copies bear this notice and the full citation on the first page. Copyrights for components of this work owned by others than ACM must be honored. Abstracting with credit is permitted. To copy otherwise, or republish, to post on servers or to redistribute to lists, requires prior specific permission and/or a fee. Request permissions from permissions@acm.org.

MobiSys '17, June 19–23, 2017, Niagara Falls, NY, USA

© 2017 ACM. ISBN 978-1-4503-4928-4/17/06...\$15.00

DOI: <http://dx.doi.org/10.1145/3081333.3081358>

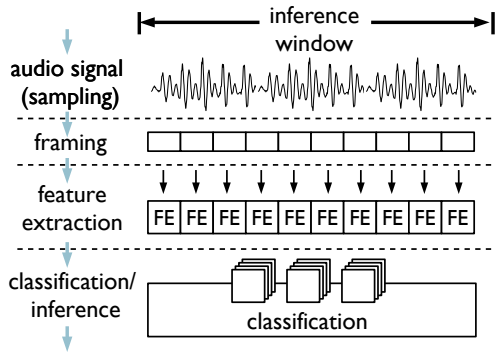


Figure 1: Audio pipeline structure.

with some preliminary optimization. The batching delays required for the benefits to appear are sufficiently short to support the operation of not only life-logging style behavior monitoring applications that tolerate large delays, but also apps that deliver context aware services and notifications such as conversation analysis [58, 43].

The contributions of our work are:

- A detailed study of the trade-offs of using mobile system-on-a-chip GPUs for audio sensing workloads.
- An optimization engine that uses key structural and memory access parallel patterns applicable to popular algorithm building blocks used in numerous audio sensing apps available commercially and in the literature. These patterns allow us to automatically tune the GPU performance boost of audio pipelines: they 1) increase the data parallelism by allowing a larger number of threads to work independently on smaller portions of the audio input stream; and 2) strategically place data needed by the threads into GPU memory caches where access latency is lower and the data can be reused.
- A comprehensive proof-of-concept OpenCL [11] implementation of widely used audio sensing algorithms built on a smartphone development board [15]. Our prototype includes a library of sensing components for feature extraction and classification (including DNNs [34], GMMs [18] etc.) needed for common forms of context inference. These components serve as the building blocks for numerous apps from the audio processing literature – as a demonstration, we implement 3 recently proposed application pipelines (e.g., emotion recognition, speaker identification and spoken keyword spotting).

To the best of our knowledge, we are the first to identify generalizable GPU parallel optimizations that are *applicable across multiple algorithms* used in the unique workloads required by audio sensing. Previous efforts [60, 29] have focused on different workload scenarios (e.g., automated speech recognition) where processing requirements differ from those imposed by audio sensing: continuous background monitoring of coarse sound classes supported by offline-trained models that can operate entirely cloud-free.

2. AUDIO SENSING MEETS THE GPU

In this section, we detail the operation of typical microphone-based sensor apps, elaborate on the GPU execution model and highlight some of the challenges it presents for audio sensing.

2.1 Audio Sensing Primer

Audio sensing apps are characterized by their ability to sample and process microphone data – they include specialized audio processing code that is distinctly different from the app specific logic

(e.g., activating services based on detected audio context). The dataflow of sensor processing within these apps share many similarities which we illustrate in Figure 1. The execution begins with the sampling of the microphone where raw data is typically accumulated over a short time window (hundreds of milliseconds up to a few seconds) sufficient to capture distinctive characteristics of sounds and utterances. The audio signal is then subdivided into much shorter (e.g., 30ms) segments called *frames* which are subject to preprocessing and feature extraction. The aim of the features is to summarize the collected data in a way that describes the differences between targeted behavior or context (e.g., sounds, words, or speaker identity). Identifying which activity or context is observed in the sensor data in the analyzed time window requires the use of one or more classification models. Models are usually built offline prior to deploying a sensor app based on examples of different activities and often the classification (i.e., model evaluation applied to the whole window of stacked frame feature data) is a bottleneck stage of the audio pipeline [27]. Example audio apps with their execution properties are listed in Table 1.

2.2 Example Audio Applications

Two most widely used classification models in the audio sensing domain are Gaussian Mixture Models (GMMs) and Deep Neural Networks (DNNs). Table 2 gives instances of their near ubiquitous usage. Here we describe the operational semantics of 3 representative data-intensive deep-inference examples built on these models. However, we note that the techniques we develop are applicable to any other audio sensing application from Table 2 that uses these models as a building block.

Speaker Identification (GMM based). The pipeline is introduced by Rachuri et al. [52]. Gaussian Mixture Model classifiers are trained using speech from 23 speakers. Each of the speakers is represented by a speaker-specific GMM built by performing Maximum a Posteriori (MAP) adaptation of a 128-component background GMM representative of all speakers. The GMM evaluates the probability with which certain acoustic observations match the model and in our case these observations are 32 Perceptual Linear Prediction (PLP) coefficients [32] extracted from 30-ms frames over 5 seconds of recorded audio. At runtime, the likelihood of the audio sequence is calculated given each speaker model and the speaker with the highest likelihood is predicted.

Emotion Recognition (GMM based). Structurally, the pipeline is identical to the Speaker Identification. The difference comes from the parameters of the GMMs which are trained on a different dataset (the Emotional Prosody Speech and Transcripts library [44]) so that each GMM represents an emotional category [52].

Keyword Spotting (DNN based). The application is based on the small-footprint implementation of Chen et al. [22], and its aim is to detect a hot phrase spoken by a nearby speaker. The example application is trained to detect an "Ok, Google" command. The audio analysis is performed by segmenting the input signal into frames of length 25ms with an offset of 10ms, i.e. the frames overlap. Filter-bank energies (40 coefficients) are extracted from each frame and accumulated into a group of 40 frames. The features from these frames serve as the input layer to a DNN with as many output layer nodes as there are target keywords (plus an additional sink node to capture other words). The DNN is fully connected and has 3 hidden layers with 128 nodes each. The output of the DNN is raw posterior probabilities of encountering each of the keywords over the last second of data. The DNN feed forwarding is performed in a sliding window with every new frame, resulting in 100 propagations per second (once every 10 ms).

Application	Purpose	Main Features	Inference Model	Frame	Window
Emotion Recognition* [52]	emotion recognition	PLP* [32]	14 Gaussian Mixture Models* [18]	30ms	5s
Speaker Identification* [52]	speaker identification	PLP*	23 Gaussian Mixture Models*	30ms	5s
Keyword Spotting* [22]	hotphrase recognition	Filterbank Energies*	Deep Neural Network* [34]	25ms	1s
Stress Detection [46]	stress from voice	MFCC [26], TEO-CB-AutoEnv [61]	2 Gaussian Mixture Models*	32ms	1.28s
Speaker Count [58]	speaker counting	MFCC, pitch [25]	Unsupervised Clustering	32ms	3s
Ambient Sound Classification [47]	sound recognition	MFCC, Time Domain Features	Gaussian Mixture Models*	64ms	1.28s

Table 1: Example audio sensing applications and their properties. * Apps and models implemented in OpenCL.

Classifier	Applications
GMM	emotion recognition [52], speaker identification [52, 45], ambient sound classification [47], stress detection [46]
DNN	keyword spotting [22], emotion recognition [30], speech recognition [33], sound event classification [49]

Table 2: Categorization of audio sensing applications based on classification model.

Pattern	Type	Applicability
fan-out	structural	GMM, DNN, feature extraction sub-phases
vectorization	memory access	ubiquitous
sliding window	memory access	DNN, pre-emphasis
tiling	memory access	GMM, filter banks

Table 3: Parallel optimization patterns taxonomy.

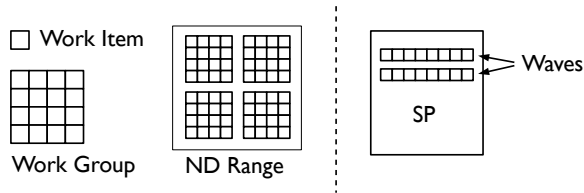


Figure 2: OpenCL thread model and a GPU Shader Processor. The SP features 2 waves of 8 work items each, it can run 16 threads in total simultaneously. The work items of one work group are executed on a single SP.

2.3 GPU Execution Model and Challenges

We use OpenCL’s terminology [11] and Qualcomm Adreno GPU [12] as an example for GPU architecture and programming model, but our discussion and conclusions apply equally to other GPU platforms, such as NVIDIA with CUDA [9]. To an OpenCL programmer, a computing system consists of a *host* that is traditionally a CPU, such as the Snapdragon 800 Krait CPU, and one or more *devices* (GPU) that communicate with the host to perform parallel computation. Programs written in OpenCL consist of host code (C API extensions) and device code (OpenCL C kernel language) – communication between the two is performed by issuing commands to a command queue through the host program space. Example commands are copying data from host to device memory, or launching a *kernel* for execution on the device. Kernels specify the data-parallel part of the program that will be executed by the GPU threads. When a kernel is launched, all the threads execute the same code but on different parts of the data.

Thread Model and Compute Granularity. All the threads generated when the kernel function is called are collectively known as a grid (or ND Range) and are organized in a two-level hierarchy independently from the underlying device architecture. Figure 2 illustrates this organization. The grid consists of *work groups* each containing a set of threads known as *work items*. The exact thread scheduling on the GPU is decoupled from the work groups and is vendor specific although it shares a lot of similarities among GPU varieties. Switching from a group of work items to another occurs when there is a data dependency (read/write) that must be completed before proceeding and is done to mask these IO latencies.

One of the challenges of implementing GPU-friendly algorithms is providing the right level of work item granularity. If the GPU threads are too few, the GPU will struggle with hiding memory access latency due to not being able to switch between compute-ready threads while others are stalled on a memory transaction.

Audio sensing algorithm execution revolves around the analysis of frames, and a natural candidate for data parallelization is to let each work item/thread analyze a frame. However, the number of frames in an inference window is on the order of tens to hundreds, whereas the GPU typically requires thousands of threads for any meaningful speedups to begin to appear. A challenge is organizing the audio algorithm execution in a way that allows more work items to perform computation.

Managing Memory-Bound Audio Kernels. Work items have access to different memory types (global, constant, local/shared, or private) each of which provides various size vs. access latency trade-offs. Global memory is the largest but also the slowest among the memories. Private memory is exclusive to each work item and is very limited in size, whereas the shared memory is larger and accessible by all work items in a group. Often, a *compute to global memory access (CGMA) ratio* is used as an indicator of the kernel efficiency – the higher the ratio is, the more work the kernel can perform per global memory access, the higher the performance.

Typical algorithms used in audio sensing need to read a large number of model parameters which they apply to the frame data, but the number of floating point operations per read is relatively low making audio kernels *memory-bound*. In order to squeeze maximum performance out of the mobile GPU (highest speed and thus lowest energy consumed), algorithms will need to reduce the global memory traffic by intelligently leveraging the smaller but lower access latency memories (shared and private). The challenge is enabling appropriate memory optimization strategies that keep the CGMA ratio high while maintaining a suitable level of granularity for the work items.

Summary. GPUs are a powerful platform for general-purpose computing programmed by language abstractions such as OpenCL and CUDA. An unanswered challenge is how and what performance control techniques we can leverage that depend on the algorithm semantics rather than a concrete hardware configuration.

3. OPTIMIZATION ENGINE OVERVIEW

To address the GPU deployment challenges presented in the previous section, we build a library of OpenCL auto-tunable audio routines that form the narrow waist of audio processing pipelines found in the mobile sensing literature (e.g., filter bank feature extraction, Gaussian Mixture Model, Deep Neural Network inference). This library builds upon a set of structural and memory access techniques that expose a set of tunable audio model-dependent *control-flow parameters* which we can control in a pre-deployment step

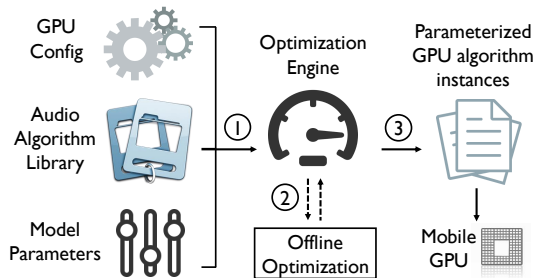


Figure 3: High-level optimization engine workflow.

with an optimization engine. The goal of this engine is to provide the best match between the domain-specific library implementation and mobile GPU hardware constraints. The engine helps to avoid cumbersome hand tuning, instead automatically finds optimal parameters for the audio kernel routines with large performance boosts for some of the algorithms. This requires *zero* change in the kernel code itself, the parameters are passed through OpenCL commands as kernel arguments at runtime. A high-level workflow is illustrated in Figure 3.

The pre-deployment step is a three-staged process, where the engine first loads as input audio model parameters such as the DNN layout and queries the GPU device specification (e.g., GPU shared cache size) in order to be able to estimate optimum values for the GPU algorithm control-flow parameters. In the second stage, the engine performs the optimization step by solving a series of linear and quadratic equations and outputs a configuration file with GPU-kernel parameter values required by our audio library. The third stage is loading the values from the locally persisted config file to parameterize the audio algorithms upon initialization of concrete sensor apps.

To provide high-performance parallel implementations, we build the techniques listed in Table 3 that enable control over the following parameters. Empirically we found that for memory-bound audio kernels, these provide a sweet spot of tunable but not too complex parameters with a key impact on mobile GPU performance:

- **frame fan-out factor** (ϕ) – defined as the total number of audio frame processing GPU threads. A higher value results in an increase in the number of concurrent threads that can work independently.
- **per-thread compute factor** (κ) – defined as the number of computed output values per GPU thread. By optimizing this the engine attempts to maximize the number of computations each thread can perform relative to its memory reads and writes (favoring compute-bound operation instead of memory-bound).

Manipulating the first parameter is achieved in our library through the *frame fan-out* structural optimization pattern. The core idea behind it is to split the audio analysis so that each GPU thread can work on a subset of the output values extracted from an audio frame. The second parameter is tightly related to a set of memory access patterns that reduce expensive global memory traffic and increase the per-thread compute factor. These techniques are: 1) *Vectorization* that consolidates slow global memory reads into a single load operation which is possible thanks to the sequential nature of accessing values from the audio stream. In our examples, the engine selects larger read batches and can fetch into the thread registers up to x values from memory, where x is vendor specific (for Qualcomm Adreno $x = 16$, for NVidia Tegra X1 $x = 4$ [10]). 2) *Memory Sliding Window* and *Memory Tiling*: the techniques allow threads to collaboratively load data into shared memory where this

data can be subsequently reused with lower latency to produce multiple output values. These are critical optimizations since global memory access is arguably the most prominent bottleneck we observe in the widely used audio classification and feature extraction algorithms.

4. PARALLEL CONTROL-FLOW OPTIMIZATION

In this section, we detail the structural and memory access parallel patterns that enable the optimization engine to parameterize the audio routines in our library.

4.1 Inter- and Intra- Frame Fan-Out

This pattern controls the level of data parallelism by allowing a larger number of concurrent threads to perform independent computations on the input data. We can support such a mode of operation thanks to the way audio pipelines process frames – repeatedly mixing the frame samples/coefficient with multiple parameters (GMM mixtures, DNN network weights). Independent computations are performed not only among different frames but also within a single frame as well, a phenomenon which we call the *frame fan-out*. This allows the total amount of threads, or *fan-out factor* (ϕ), to be relatively high. It can be computed as follows: $\phi = \frac{n \cdot \nu}{\kappa}$ where n is the number of frames, ν is the total number of output values per frame, and κ is the number of computed values per GPU thread (*per-thread compute factor*). This structural optimization is applicable across both feature extraction (filter bank computation) and classification phases. The next two examples illustrate how this pattern can be applied:

GMM Fan-Out. The input for this classification phase is the extracted feature coefficients from all frames. In the Speaker Identification pipeline there are 32 PLP frame features and a total of $n = 500$ frames per inference window (one frame every 10ms for 5s). Each GMM has $\nu = 128$ mixtures each of which computes a probability score by mixing the 32 PLP coefficients from a frame with the parameters (mean and variance) of 32 Gaussian distributions. With a per-thread compute factor of $\kappa = 1$, we could let each OpenCL work item estimate the probability score for one mixture per frame resulting in a fan-out factor of $\phi = 500 \times 128$. We enable the kernel to generate this massive number of work items by letting them write intermediate scores to global memory and a separate kernel is launched to sum the scores.

DNN Fan-Out. Similarly, the input data for the keyword spotting DNN classification is the extracted filter bank energies from the frames. In a 1-second inference window there are a total of $n = 100$ network propagations (one per new frame every 10ms). A DNN kernel computes partial results across all input frames by performing the feed forward propagation for one layer across the frames simultaneously. Multiple kernels are launched each of which computes the node activation values for the next layer. With $\nu = 128$ nodes in the hidden layers we could let each OpenCL work item compute the activation for one node per frame offset ($\kappa = 1$) resulting in a fan-out factor of $\phi = 100 \times 128$.

The role of the optimization engine is to provide optimum values for the control-flow parameters ϕ and κ . n and ν are determined directly by the audio model specification, whereas the final value of ϕ depends on κ , or the amount of work each GPU thread is assigned. The engine tunes the per-thread compute factor κ since we observe that *maximum GPU performance may not necessarily be reached when parallelism is highest*. The fan-out factor ϕ reaches its maximum when its denominator (κ) has its lowest value ($\kappa = 1$), i.e.

Algorithm 1 Shared Memory Use Kernel Template

```
1: Input: (i) Pointer to input buffer (in), (ii) Pointer to output
   buffer (out), (iii) Thread local id (lid), (iv) Thread group id
   (gid), (v) Shared memory maximum size (max_s).
   ▷ Collaborative data load:
2: loadOffset ← compute_load_offset(lid)
3: inputOffset ← compute_input_offset(gid, lid)
4: shared floatN data[max_s] ▷ shared memory declaration
5: if loadOffset < max_s then
6:   data[loadOffset] ← vloadN(0, &in[inputOffset]) ▷
   vectorized
7: barrier(CLK_LOCAL_MEM_FENCE) ▷ wait for all threads
   to finish loading data
   ▷ Shared data processing:
8: for (i = 0; i < x; ++ i) do
9:   localDataOffset ← compute_local_offset(lid, i)
10:  result ← process(&data[localDataOffset])
11:  outputOffset ← compute_output_offset(gid, lid, i)
12:  out[outputOffset] ← result
```

when there are more threads performing less work. The memory access patterns in the following subsection enable each GPU thread to perform more computation ($\kappa > 1$) relative to the number of its memory reads and writes: the total count of threads decreases but they can make a more efficient use of memory.

4.2 Memory Access Control

Tuning audio kernel performance with the per-thread compute factor κ is closely related to how memory access is managed by the threads in a work group. Increasing the number of computations per thread per global memory access and thus finding optimum values for κ depends on maximum exploitation of the faster but limited in size GPU memories. We discuss several key strategies, enabled by the specifics of digital signal processing, to lower the number of global memory operations. These strategies either 1) batch global memory transactions into fewer operations, or 2) let the threads in a work group collaboratively load data needed by all of them into shared memory where access latency is lower.

Vectorization. When kernels read the input data features or parameters, for instance, they access all the adjacent values in a frame. As a result, the memory access can be vectorized and consolidated with vector load operations that fetch multiple neighboring values at once from global to private memory. For example, when a thread requires the 32 PLP coefficients from a frame, it can use the OpenCL *vloadx* operation to issue 2 reads with 16 values (*vload16*) fetched simultaneously instead of performing 32 reads for each coefficient separately.

Shared Memory Sliding Window. Often the input raw audio or feature stream is processed in sliding window steps, i.e. the input is divided into overlapping frames over which identical computations are performed. Example scenarios where this type of processing is commonly applied are the feature extraction (PLP, MFCC [26]), or the classification of the feature stream into observed phenomena (as is the case for the DNN keyword spotting, see Figure 4). The data overlap is usually quite substantial – the feature extraction phase for the Speaker Identification pipeline, for instance, uses 30ms frames (240 samples at a sampling rate of 8kHz) with a 10ms frame rate (an offset of 80 samples) resulting in a 66% data overlap between subsequent frames. We can exploit this property of the audio stream processing to let the threads in a work group collaboratively load a larger chunk from the input spanning samples from multiple frames into shared memory (where access latency is lower), and let each thread reuse its loaded parameters by applying

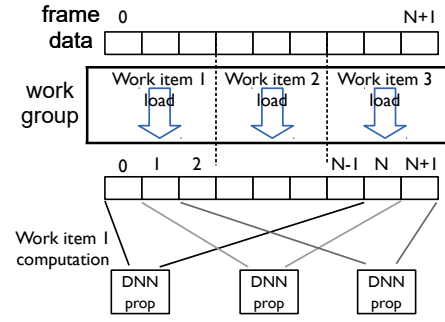


Figure 4: Sliding window example. The DNN activation of one node in the first layer (denoted by DNN prop) is performed by each work item in a work group. The required data for one such computation is N frames. The figure explicitly shows the computation for work item 1 which is performed for 3 frame offsets from the accumulated frame input data (0 to $N - 1$, 1 to N , and 2 to $N + 1$). Each work item in a group can load a part of the data needed for the DNN layer activation, but will use all data loaded by the peers in the group, as work item 1 does. A work item computes the activation for one node in a layer (DNN prop), but since more data is accessible from the collaborative loading, the item can reuse its parameters to compute the activation for the same node for 3 different frame offsets.

them against several offsets from the input. The higher the data overlap for adjacent frames, the larger the opportunity the threads have to load more adjacent regions with fewer read operations, and the more computation they can perform per global memory read. The pattern enables the control of the per-thread compute factor κ by increasing the CGMA ratio of the kernel operation.

Algorithm 1 shows example kernel pseudo code where the work items cooperate to load data into shared memory. The key advantage is that each thread can use a single vectorized fetch which is only a small proportion of the actual data needed from global memory. Collectively, however, all threads are able to load the data needed by their peers in the work group. The number of adjacent input regions x over which the threads in a work group perform computations are limited by the maximum size of the shared memory reserved to a work group. For Adreno 330 that size is 8KB. The optimization engine estimates the maximum x as a function of the model size and shared memory constraints, the pattern exposes x as the per-thread compute factor ($\kappa = x$).

Shared Memory Tiling. As discussed in the description of the frame fan-out in §4.1, when audio processing pipelines work on a frame they usually produce multiple output values (e.g., feature coefficients or probability scores) by combining the frame data with multiple parameters. The procedure can be treated as *generalized dense matrix-matrix multiplication* with the two matrices being: 1) an input matrix $I_{(n,d)}$ with n input frames each of which has d elements (samples/coefficients); and 2) a parameter matrix $P_{(k,d)}$ with k parameters each of which has dimensionality d . The result of the combination of the two matrices is a matrix $O_{(n,k)} = I_{(n,d)} \otimes P_{(k,d)}^T$ where \otimes can be a generalized operation that performs a reduction over d elements from the two matrices (a row from O and a column from P^T). Prominent applications of this operation can be found in the computation of the filter bank coefficients, the GMM mixture probability estimation, and the DNN network propagation. An example reduction \otimes used in the GMM classification stage is shown in the following equation:

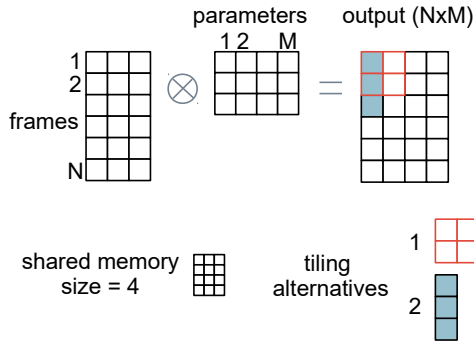


Figure 5: Tiling example. There are N frame data rows and M parameter columns that can be combined to yield $N \times M$ output values. The shared memory size of a work group is limited to 4 frame rows or parameter columns in total. There are 2 tiling alternatives. Alternative 1 fills shared memory by loading data for 2 frames and 2 parameters leading to 4 computed values in total from the work group. Alternative 2 loads data for 3 frames and 1 parameter leading to 3 computed values in total.

$$o_{ij} = -\frac{1}{2}(g_j + \sum_{0 \leq s < d} (x_{is} - m_{js})^2 v_{js}) \quad (1)$$

where o_{ij} is one element from the output matrix; m_j , v_j , and g_j are the Gaussian parameters of a mixture component; and x_i are feature values from frame i .

The straightforward implementation of a GPU kernel to compute matrix O would be to let each thread compute one output value o_{ij} and O independently an input row i and a parameter column j . However, a strategy for reducing global memory traffic is to introduce a model-specific version of *tiling algorithms* used in matrix-matrix multiplication [39]. The core idea is to let the work groups of a kernel partition the output matrix into *tiles* so that the total data for each tile fits into shared memory. Our goal is to have the threads in a work group collaboratively load both input data and parameters into shared memory in a way that maximizes the number of computations per global memory read. This can be achieved if the number of computed values ($\{\text{number of frames}\} N_f \times \{\text{number of parameters}\} N_p$) per loaded data is as large as possible for the entire work group. Figure 5 illustrates the pattern in operation.

4.3 Parameter Estimation

We calculate key optimization parameters as described below.

Vector size x . The engine selects the vector size for batched memory reads by querying with OpenCL commands whether the audio kernel can successfully be compiled with the given value for x . The engine enumerates the possible values for x in descending order and picks the highest value under which the kernel successfully compiles. Compilation may fail when the size of the vectorized loads exhausts the thread register space.

Memory sliding κ . Optimizing this parameter involves solving a linear equation with respect to the GPU shared memory size, and input model parameters. If S_M is the total number of values the shared memory can accommodate, S_F is the input region size, and r is the frame offset in number of input values, then the maximum κ is computed in the following manner: $\kappa = \left\lfloor \frac{S_M - S_F}{r} \right\rfloor + 1$.

Memory tiling κ . The optimization engine makes a two-staged decision: whether to activate this pattern and if activated how to best parameterize it. The decision is based on the type of the model

used for audio analysis (filter banks, GMM, or DNN), input model dimensions (size of the model parameters), maximum work group size, and shared memory size. The optimization engine estimates the work group size and an optimum number of output matrix values each thread in the work group should compute so that global memory accesses are minimized. This is implemented by solving a quadratic equation with respect to N_f and N_p under the shared memory constraints. In our examples, the pattern would be activated for the filter banks and GMM computation, but not for the DNN where the size of the network is prohibitively large for any meaningful subset to be effectively exploited from shared memory.

Frame fan-out ϕ and work group size. The engine estimates the fan-out factor in a final step by reading the specified audio model parameters (e.g., number of frames) and having κ determined in a prior step. We strive to select the largest work group size possible. Similarly to vectorization, this can be done by exhaustively trying to compile the kernels with values up to the maximum size allowed. Sizes are enumerated in multiples of the *preferred group multiple parameter* (queried from the GPU with OpenCL).

5. IMPLEMENTATION

We briefly summarize the details of the software artifacts used in this work.

Hardware and APIs. We prototype the audio sensing algorithms on a Snapdragon 800 Mobile Development Platform for Smartphones (MDP) [15] with an Android 4.3 Jelly Bean OS featuring Adreno 330 GPU present in mobile phones such Samsung Galaxy S5 and LG G Pro2. All GPGPU development is done with OpenCL 1.1 Embedded Profile and we reuse utilities for initializing and querying the GPU from the Adreno SDK that is openly available [12]. In addition, we prototype baseline versions of the audio sensing pipelines for the Qualcomm Hexagon DSP [13] with the Hexagon C SDK v1.0 [14]. The DSP has 3 hardware threads and we use the *dspCV* thread pool library shipped with the Hexagon SDK to build multithreaded versions of the algorithms for the DSP. The CPU sequential baselines reuse the C code built for the DSP and are accessed by interfacing with the Android Native Development Kit (NDK). Multithreaded CPU versions are built by using C++11 threads – we leverage the 4 cores available to the Snapdragon Krait CPU. Note, our implementation does not explicitly leverage, nor is structured for the use of, SIMD instructions (like NEON) as available in the Krait CPU. Although we take advantage of Qualcomm SDK primitives and other best practices (described next) that enhance the performance of the CPU and DSP in the Snapdragon. Power measurements are performed with a Monsoon Power Monitor [8] attached to the MDP. Classifier models are trained with the HTK toolkit [6] for the Speaker/Emotion Recognition and the Theano python library [17] for the Keyword Spotting.

DSP Baseline Implementation. We implement basic DSP benchmarks as a ballpark reference on energy consumption and a first indication of latency when machine learning algorithms found in audio sensing are executed on a low-power chip. As stated above, we use the Qualcomm Hexagon SDK to tailor implementations to the DSP which are not a direct compilation of CPU-based code. The DSP C language features are a subset of the standard C distributions [27], which is why without significant modifications most CPU algorithms cannot be directly executed on the Hexagon DSP. Instead, we build our baselines to match the requirements and conventions of the Hexagon Elite SDK for audio processing, our basis is DSP-targeted code which has been modified to be executed on the CPU as well. Although we have yet to take advantage of

the more advanced VLIW (Very Long Instruction Word) instructions available to the DSP everywhere in our code, our DSP implementations are not naive CPU-variants as we reuse some of the optimized DSP processing routines coming readily with the DSP SDK (such as FFT computation): these already come with VLIW optimized instructions and intrinsics. The algorithms that are not included in these DSP libraries we have implemented ourselves following the guidelines provided by the Elite audio processing SDK (e.g., for memory allocation). We acknowledge additional research is needed to find the most optimal DSP implementations, however we do leverage optimized algorithmic primitives distributed with the SDK to give some reference numbers on the amount of energy required to process machine learning algorithms found in audio sensing.

Kernel Compilation. Building the OpenCL kernels can be done either via reading the sources from a string and compiling them at runtime or by pre-compiling the source into a binary. We use pre-compiled binaries that drastically reduce the kernel load time and that need to be produced once per deployment.

6. EVALUATION

In this section, we provide an extensive evaluation of the parallel optimizations under representative audio sensing algorithms when deployed on a mobile GPU. The main findings are:

- Optimizing the control-flow parameters is critical – naively parameterized GPU implementations may be up to 1.5x slower than multithreaded CPU baselines and consume more than 2x the energy of offloading batched computation to the cloud.
- The total speedup against a sequential CPU implementation for an optimized GMM-based and a DNN-based pipeline running entirely on the GPU is 8.2x and 13.5x respectively, making the GPU the processing unit of choice for fast real-time feedback. The optimized GPU is also 3-4x more energy efficient than sequential CPU implementations, but can consume up to 3.2x more energy than a low-power DSP.
- After a certain batching threshold (10 to 20 seconds) of computing multiple inferences in one go, optimized GPU algorithms begin to consume less energy than cloud offloading with good throughput (5Mbps and 10Mbps), in addition to obtaining inferences 3.1x and 6.5x times faster for the GMM and DNN-based pipelines respectively.
- The total energy consumption under batching scenarios is in ranges comparable to those delivered by reference low-power DSP implementations with some basic optimization.

6.1 Experimental Setup

Experiments are performed with the display off and the algorithms are executing in the background, as is typical for sensing apps to operate in such mode. We denote with *Audio Optimized GPU (a-GPU)* the output from the optimization engine as described in §3. Throughout the section we use the following baselines.

- *DSP sequential (DSP).* Our DSP baselines are implemented as specified in Section 5 via the Hexagon DSP in DSP-compatible C. We reuse optimized built-in primitives for FFT computation, memory allocation and follow the conventions of the Elite SDK for audio processing. Our implementations are meant to be used as a ballpark reference on the energy efficiency that can be supported by low-power units but do not claim they are the most efficient that can be achieved through advanced hardware optimizations applied rigorously throughout the code base.

Computation	Parameters	Speed-up Gain
GMM	$x = 1, \kappa = \nu$	3.6x
	$x = 16, \kappa = \nu$	12.8x
	$x = 16, \kappa = 1$	15.6x
	$x = 16, \kappa = 4$ (tiling)	16.2x
DNN	$x = 1, \kappa = \nu$	1.8x
	$x = 16, \kappa = \nu$	4.8x
	$x = 16, \kappa = 1$	13x
	$x = 16, \kappa = 5$ (sliding window)	21.3x
Filter banks	$x = 1, \kappa = \nu$	1.7x
	$x = 16, \kappa = \nu$	4x
	$x = 16, \kappa = 1$	6x
	$x = 16, \kappa = 2$ (tiling)	6.6x

Table 4: Parameter configuration speed-ups vs. CPU sequential implementation. Lines in bold show the optimal parameter values found by the optimization engine.

- *CPU sequential (CPU).* Our implementations have a sequential workflow that follows the DSP code structure but reimplements some of the routines that require DSP-specific VLIW instructions (e.g., FFT computation). The baselines are based on DSP-compatible C.
- *CPU multi-threaded (CPU-m).* We implement variants of the pipeline algorithms where the bottleneck classification stage of the audio pipeline (occupying > 90% of the runtime in our examples) is parallelized across multiple threads. The GMM classification is restructured so that each GMM model probability is the unit of work for a separate thread. We maintain a pool of 4 threads which equals the number of physical cores of the Snapdragon Krait CPU – adding more threads did not lead to any performance benefits. The DNN classification is restructured so that the network propagation step is performed in parallel: each thread processes the activation of one node in a layer.
- *DSP multi-threaded (DSP-m).* Similarly to the multi-threaded CPU versions of the algorithms, we adopt DSP alternatives that parallelize the pipeline classification. The parallel DSP variants have logically the same threading model as the CPU one, with the difference that the DSP thread pool size is 3, i.e. it equals the number of hardware threads. We use the worker pool utility library *dspCV* which speeds up the execution for Computer Vision algorithms on the DSP.
- *Naive GPU (n-GPU).* We add the most naively parameterized GPU implementations as explicit baselines in addition to showing different parameter configurations. For all algorithmic building blocks (GMM, DNN, and features) in this naive baseline category we set the vectorized load factor $x = 1$, and the per-frame compute factor to be $\kappa = \nu$ which results in a frame fan-out factor of $\phi = n$.

Energy Measurements. All energy measurements are taken with a Monsoon Power Monitor attached to our MDP device. By default, the experiments were performed with a display off, with no services running in the background except system processes. This reflects the case when GPU offloading is done in the background, as in a continuous sensing scenario. The power evaluation setup closely matches the one reported by LEO [28]. Each application is profiled separately for energy consumption by averaging power over multiple runs on the CPU, DSP and GPU.

6.2 Pattern Optimization Benchmarks

In this subsection, we study how the application and parameterization of the various optimization techniques presented in §4

	GMM full pipeline	GMM classification	DNN full pipeline	DNN classification
DSP	-8.8x	-8.6x	-4.5x	-4.0x
DSP-m	-3.2x	2.5x	-2.1x	-1.5x
CPU (runtime)	1.0x (1573 ms)	1.0x (1472 ms)	1.0x (501 ms)	1.0x (490 ms)
CPU-m	3.0x	3.4x	2.8x	2.9x
n-GPU	3.1x	3.6x	1.8x	1.8x
a-GPU	8.2x	16.2x	13.5x	21.3x

Table 5: Speedup factors for one run of the various pipeline implementations compared against the sequential CPU baseline. Negative numbers for the DSP variants show that the runtime is that amount of time slower than the CPU baseline. CPU average runtime in ms is given for reference in brackets. Note that the DSP numbers are provided by our reference implementation under the conditions specified in the baseline definition. A highly optimized DSP implementation might challenge the CPU latency-wise in certain scenarios. We still expect the a-GPU to be the lead given its current massive speed-ups.

affect the GPU kernel runtime performance. Table 4 shows different points in the parameter space compared to the engine optimized configuration.

Pattern Speedups. A first observation is that using vectorization with larger batches ($x = 16$) provides a significant boost across all algorithms. The speedup of the most naive GMM kernels jumps from 3.6x to 12.8x, the DNN ones – from 1.8x to 4.8, and the filter banks – from 1.7x to 4x. The success of this simple technique can be attributed to the fact that the mobile GPU is optimized to efficiently access multiple items with a single instruction.

Another observation is that increasing the fan-out factor ϕ by setting $\kappa = 1$ provides tangible runtime boosts. As illustrated, speedups increase from 12.8x to 15.6x for the GMM, and from 4.8x to 13x for the DNN. Interestingly, the higher fan-out provides benefits even though the number of global memory accesses is raised by issuing writes of intermediate values to a scratch memory. The reason for this is that the fan-out pattern prominently increases the total number of work items and as a consequence there are more opportunities for the GPU to hide memory access latencies – whenever a group of threads is stalled on a memory read or write operation, with a higher probability the GPU can find another group that can perform computation while the former waits.

Last but not least, the more advanced tiling and sliding window techniques tuned by the optimization engine provide noticeable speedup improvements over the straightforward use of shared memory. The sliding window optimization boosts the second best DNN kernel speedup from 13x to 21.3x, which is also the highest cumulative gain observed across all algorithms. Optimally parameterized tiling, on the other hand, brings the overall GMM speedup to 16.2x and filter banks to 6.6x. In these cases, increasing κ further results in suboptimal use of shared memory – since its size is limited, the work items can fetch only a proportion of the total data they need, the rest needs to be loaded from the slower global memory into thread registers.

Summary. The engine optimized kernels allow GPU computation to exhibit much higher performance than naively parameterized baselines. The optimization techniques can be ubiquitously applied across multiple stages of the pipelines.

6.3 GPU Pipeline Runtime and Energy

We compare our engine optimized GPU pipelines against the baselines listed in §6.1. Table 5 shows the runtime for running the pipelines on the various processing units. The most prominent observation is that the optimized GPU implementation is the fastest one. For instance, the full GMM and DNN pipelines are 8.2x and 13.5x times faster than a sequential CPU implementation respectively, an order of magnitude faster. In comparison, the CPU multi-threaded alternatives are around 3x times faster only. If the GPU

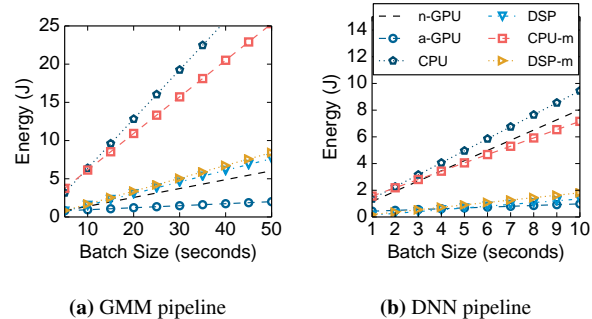


Figure 6: Energy (J) as a function of the audio processing batch size in seconds. Legend is shared, axis scales are different.

is not carefully utilized, the naively parameterized GPU implementations may be up to 1.5x slower than the multicore variants (e.g., DNN pipeline). The reason why the audio-optimized GPU fares so much better than both multicore CPU and naive GPU alternatives is because massive data parallelism is enabled by the parallel techniques – the hundreds of cores on the GPU can work on multiple small independent tasks simultaneously and hide memory access latency. This is especially true for the classification tasks that are 16.2x (GMM) and 21.3x (DNN) faster than their sequential CPU counterparts.

In Figure 6 we plot the energy needed by the various units to execute the pipeline logic repeatedly on batched audio data. For one-off computations the cheapest alternative energy-wise is the DSP which can be up to 3.2x more energy efficient than the optimized a-GPU for the DNN pipeline. Yet, the a-GPU is between 3x and 4x times more energy efficient than the sequential CPU for both applications. *If high performance is of utmost priority for an application, the GPU is the method of choice for on-device real-time feedback* – when optimized, GPU offloading will obtain inferences much faster and significantly reduce energy compared to the CPU.

A notable observation is that as the size of the buffered audio data increases, the a-GPU begins to deliver energy efficiency in the ranges provided by the low-power DSP. For instance, with batch sizes of 10 and 6 seconds for the GMM and DNN pipeline respectively, the a-GPU provides comparable energy while being multiple times faster ($> 50x$ compared to our reference baselines). If applications can tolerate small delays in obtaining inferences, batched GPU computation will save amounts of energy similarly to a low-power DSP and at the same time obtain results faster. We note that a heavily optimized DSP implementation will be the best option energy-wise; here we show that contrary to conventional wisdom, there is a scenario in which the GPU can be used to save energy on a scale that is much closer to what a low-power unit can achieve.

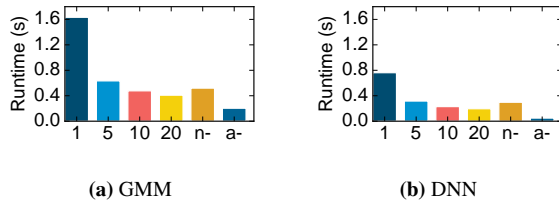


Figure 7: End-to-end latency for computing the audio pipelines on the GPU vs cloud. Numbers on the x axis show throughput in Mbps, and n- and a- refer to n-GPU and a-GPU.

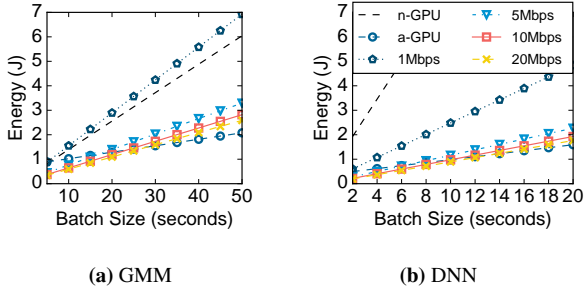


Figure 8: End-to-end energy as a function of the batch computation size for running the audio pipelines on the GPU vs cloud offloading. Legend is shared.

6.4 GPU Sensing vs Cloud Offloading

Cloud baselines. We compare the performance of the sensing algorithms on the GPU against the best performing cloud alternatives. For the DNN-style Keyword Spotting application, the cheapest alternative is to send the raw data directly for processing to the cloud because the application generates as many features as the size of the raw input data. For the GMM-style Speaker Identification pipeline, the cheapest alternative is to compute the features on the DSP and send them for classification to the cloud. However, this variant is > 10 times slower than computing the features on the CPU. Further, we find that when sending the features to the cloud, establishing the connection and transferring the data dominate the energy needed to compute features on the CPU. For this reason, the GMM cloud baseline in our experiments computes features on the CPU and sends them for classification to a remote server.

Latency Results. In Figure 7 we plot the end-to-end time needed to offload one pipeline computation to the cloud and compare it against the total time required by the GPU to do the processing (including the GPU kernel set-up and memory transfers). We assume a window size of 64KB and vary the network RTT so that the throughput ranges from 1 to 20Mbps. Given this, the a-GPU implementation is 3.1x and 6.5x faster than the good 5Mbps cloud alternative for the GMM and DNN pipelines respectively. This comes at the expense of a 1.6x and 1.4x increase in the energy for a one-off computation for the two pipeline types respectively. The takeaway is that *if speed is favoured over energy, the GPU should be used for local processing because it will deliver inference results several times faster than cloud offloading even with good connectivity.*

Energy Results. In Figure 8 we plot the total energy required to offload batched pipeline computations to the cloud as a function of the batch size in seconds for which raw audio data is queued for processing. The most notable outcome is that *the a-GPU com-*

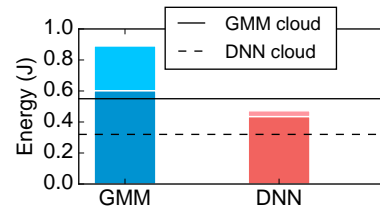


Figure 9: Energy consumed for one-off computation for the GMM- and DNN-based audio apps. Lighter shaded bars show energy spent for processing, the rest is GPU tail energy. Lines show the total energy consumed by cloud offloading for the two apps for a network connection with an RTT of 104 ms.

petes energy-wise with good connectivity cloud offloading in addition to being multiple times faster. After a certain batching threshold, the total processing with the optimized a-GPU consumes even less energy. For instance, unless the network has a throughput of 20Mbps (and an RTT of 25 ms) the GMM-style pipeline starts getting cheaper than the faster connections after 20 seconds of buffered audio, and the DNN Keyword Spotting pipeline – after only 10 seconds of audio data. The reason for this phenomenon (batched processing is less expensive than cloud and one-off computation is not) is that the initial kernel set-up and memory transfer costs are high, but once paid, the a-GPU offers better energy per second for audio sensing.

In Figure 9 we plot a breakdown of the energy for a one-time run of the audio apps on the GPU to quantify the GPU setup overhead. Overall, the amount of energy spent in the GPU tail states is over 65% of the total consumption for both applications which confirms the prohibitively high setup/tear-down GPU costs. With a network that has an average RTT of 104ms (translating to ≈ 5 Mbps throughput), the energy spent by cloud offloading is less than the GPU setup cost. Unless the audio app is highly sensitive to the runtime, cloud offloading may provide a desirable trade-off between energy and latency.

Another critical result is that optimizing GPU execution is crucial – the naive n-GPU is more expensive ($> 2x$) energy-wise than almost all types of cloud offloading when batching. With the better but still unoptimized baselines with highest fan-out ($\kappa = 1$), the batching threshold for preferring GPU execution over cloud is higher (e.g., ≈ 14 seconds for the DNN algorithm), delaying the application response time further than what could be achieved with the engine optimized version.

Summary. While cloud offloading has a significant computational lead over mobile, the GPU now provides advantages that makes local processing highly desirable – it is faster, less susceptible to privacy leaks as execution is entirely local, works regardless of connection speed, and even competes with cloud in terms of energy.

6.5 GPGPU and Graphics Workloads

Here we investigate how GPGPU computations interfere with other GPU workloads such as those used for graphics processing – *will the background GPU computation affect negatively the user experience?* We schedule the execution of the audio sensing pipelines (either Speaker Identification or Keyword Spotting) to run continuously for a minute on the GPU while the mobile user is interacting with other applications that are known to strain the GPU resources, i.e. games. We pick 5 hugely popular Android games with multi-million downloads and different play styles (Angry Birds, Fruit

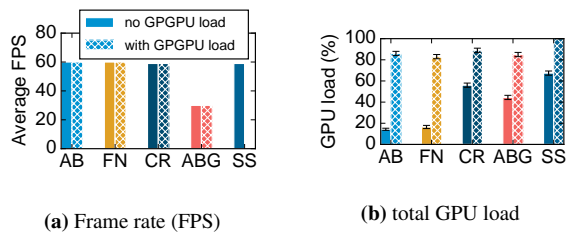


Figure 10: Average frame rate and GPU load when the games run without and with additional GPGPU load. Games in the experiment are Angry Birds (AB), Fruit Ninja (FN), Crossover Road (CR), Angry Birds GO (ABG), and Subway Surfers (SS). Legend is shared.

Ninja, Crossover Road, Angry Birds GO, and Subway Surfers), and observe the effect GPGPU computation has on the perceived game-play quality. To quantify this we measure the average frame rate (frames per second (FPS)) with GameBench [3] during gameplay over 5 1-minute long runs.

In Figure 10 we show the aggregate results from the experiments. *For all games except Subway Surfers the GPGPU computation does not change the original frame rates of the games, although the total GPU load substantially increases.* For instance, the render-heavy racing Angry Birds GO maintains an average frame rate of 30 FPS both with and without the added audio sensing workload, even though the total GPU load jumps from 44% to 85%. For this and the other three games with similar behavior (Angry Birds, Fruit Ninja, Crossover Road), the effect can be explained by the facts that 1) the original load the games place on the GPU is not too high, 2) GPU rendering is time-shared with GPGPU computation, and 3) the audio sensing kernels are short-duration (a single kernel execution never exceeds tens of milliseconds). With the endless runner Subway Surfers, however, the original average GPU load is already very high ($\approx 70\%$), and adding the GPGPU computation results in a screen freeze so that the game becomes unresponsive. This can be attributed to the fact that the OS does not treat the GPU as a shared resource and there is a lack of isolation of the various GPU workloads. One way to approach this is introduce OS-level abstractions that provide performance guarantees [53].

7. DISCUSSION AND IMPLICATIONS

Here we survey key scenarios and issues related to the applicability of the GPU parallel optimizations for audio sensing.

Targeted Scenarios. There are many chains of audio workloads that we envisage are relevant to GPU offloading with delayed cloud-free batch processing. Examples are continuous low latency audio tasks (hot key word recognition) followed by a much heavier processing that is more tolerant to the delays offered by GPU acceleration – all types of analysis possible on human voice fall into this category. There are numerous such examples of behavior monitoring in the audio sensing literature: conversation analysis [48], speaker counting [58], speaker identification [45], emotion recognition [52], and ambient scene analysis [47] to name a few. Context monitoring through sounds and triggering notifications (e.g., detect conversation to mute the speaker) is another key functionality that can be supported with this type of offloading: delayed cloud-free batch processing with entirely offline trained models, or models that need to be only infrequently updated. GPU offloading will be a crucial part of more complicated scheduling schemes that involve other processing units as well (e.g., [28]) and possibly cloud. In that case hybrid solutions that use multiple processing units and

cloud can reap the benefits of GPU execution, and more applications including those that need cloud support such as Shazam, can take advantage of the more advanced local processing (e.g., to extract the features necessary to discriminate the encountered songs).

7.1 Implications

We believe the results presented in this work provide insights of value to the following areas.

Privacy. Our findings suggest that algorithms optimized for embedded-class GPUs can bring the much coveted privacy guarantees to devices such as Amazon Echo [1] and Google Home [4], if the operation remains entirely on the device itself. These assistants respond to simple home user requests (such as, “turn on the light”), but are known to heavily exploit cloud offloading. With the help of our techniques doing the processing locally on the GPU can be done faster than cloud offloading, and without exposing sensitive information to untrusted third parties.

Servicing multi-app workloads. GPUs will play a crucial role in offloading the sensing workloads of digital assistants as they cannot be serviced by the DSP capabilities alone. Amazon Echo, for instance, performs multiple audio sensing tasks on a continuously processed audio stream, including: 1) detect the presence of speech vs other sounds; 2) perform spoken keyword spotting (as all commands are triggered by the same starting word); and, 3) speech recognition, along with additional dialog system analysis that allows it to understand and react to the command. These tasks collectively are well beyond the DSP processing and memory capabilities [27], in such multi-app audio sensing scenarios approaching the mobile GPU with routines that maximize runtime performance and minimize energy consumption is critical.

Energy reductions. Audio sensing algorithms are notorious for their continuous monitoring of the sensor stream. Whereas DSP offloading is massively adopted as the go-to power reduction approach for applications such as hot keyword spotting, with the increase in number of concurrent audio sensing services mobile users adopt (e.g., Google Now, Auto Shazam), the DSP will have to selectively process a subset of the algorithm stages. In multi-app scenarios, optimally using the GPU as we have done in this work will be instrumental in keeping the power-hungry CPU or privacy-invading cloud offloading at bay.

7.2 Discussion

Our design, and its results, also highlight the following issues.

Performance on other mobile GPU varieties. Although it is highly likely there will be a difference in the exact values for the performance boosts on other GPU models (such as NVIDIA’s Tegra), we expect qualitatively similar results when deploying the pipelines there. For example, speedups from the GPU data parallelism will be sufficiently high to deliver real-time performance for applications that can afford the energy costs. This is because our proposed optimizations can be generalized to any OpenCL-compliant GPU architecture, and do not rely on vendor-specific features.

Parallelizing other sensor processing algorithms. The core mechanics behind the optimization patterns can be applied to other classifiers such as Support Vector Machines (SVM), and deep learning network topologies such as Convolutional Neural Networks (CNN). This is because the patterns depend on how the classification is applied to the audio data stream (in sliding windows, combining model parameters with frame data independently to different frame offsets), rather than fully depend on the concrete algorithm implementation. We believe the broader lessons learned from this

work on using the GPU will promote further research into how it can be used to accelerate algorithms in other application domains (e.g., alternative sensor processing from accelerometer, or GPS).

GPU vs. multicore CPUs. As single-thread performance for microprocessor technology is leveling off, multiple cores will become major drivers for increased performance [19] (e.g., up to 61 for Intel Xeon Phi [7]). Developers will likely be faced with similar data parallel challenges – increasing the total number of concurrent tasks for better utilization, and efficiently leveraging memory caches to mask access latency. As OpenCL manages heterogeneous parallel algorithms transparently from the underlying multicore architecture, the developed OpenCL-compliant optimization techniques will prove valuable to multicore CPUs as well.

GPU programmability. GPUs are notoriously difficult to program – even if the algorithm exhibits data parallelism, restructuring it to benefit from GPU computation often requires in-depth knowledge about the algorithm mechanics. In fact, automated conversion of sequential to parallel code has been an active area of research [21, 20], but fully automating the parallelization process still remains a big challenge. We provide a portable OpenCL library of parallel implementations for key audio sensing algorithms (e.g., GMMs, DNNs) and expect developers will either compose pipelines by reusing the OpenCL host and kernel code, or by applying the insights from our optimization patterns to their implementations.

We acknowledge that currently programming GPUs requires skillful development. We hope that through our library we can simplify the pure GPU kernel development by providing optimized machine learning primitives developers can reuse. Without them, developers will mostly likely encounter the problems we uncovered while designing our library (e.g., memory-bound processing) in order to incorporate GPU processing into their audio application. We do not fully automate the process, a potential direction for future research is designing or reusing a simpler high-level declarative language that can be used to specify pipeline processing. In the case that all algorithmic components are covered by our library, this can greatly simplify the developer burden. This compiler component can be built on top of CUDA/OpenCL or industrial strength GPU APIs.

8. RELATED WORK

Our work touches most closely the following areas of research related to efficient sensing and efforts to optimize GPU usage.

Sensor Processing Acceleration and Efficiency. A large body of research has been devoted to the use of heterogeneous computation via low-power co-processors [51, 45, 27, 40, 42, 54] and custom-built peripheral devices [56] to accelerate or sustain power efficient processing for extended periods of time. Little Rock [51] and SpeakerSense [45] are among the first to propose the offloading of sensor sampling and early stages of audio sensing pipelines to low-power co-processors – the processing enabled by such early units is extremely energy efficient but limited by their compute capabilities to relatively simple tasks such as feature extraction. DSP.Ear [27] and Shen et al. [54] study more complex inference algorithms for continuous operation on DSPs but demonstrate such units can be easily overwhelmed and often the energy efficiency comes at the price of increased inference latency.

LEO [28] is a low-power scheduler that dynamically distributes computation across heterogeneous resources, including the GPU as a possible resource, and lowers the overall energy consumption for concurrent sensor apps. However, it does not investigate the trade-offs of GPU offloading in detail, nor does it show what is required to optimally utilize such a processing unit. We believe the

optimizations we designed complement sensor scheduling, and are critically needed to allow frameworks to maximize GPU usage.

General-Purpose GPU Computing. GPUs have been used as general-purpose accelerators for a range of tasks, the most popular applications being computer vision [57, 23, 36] and image processing [55, 50]. Object removal [57] and face recognition [23] on mobile GPUs have been showcased to offer massive speedups via a set of carefully selected optimization techniques. Although the techniques found in the graphics community as well as in the field of speech processing (fast spoken query detection [60]) address similar data parallel challenges to what we identify (increasing thread throughput, careful memory management), these techniques remain specific to the presented use cases.

The GPU implementation of automatic speech recognition based on GMMs [29], for example, proposes optimizations that are related to the specifics of a more complex speech recognition pipeline. Instead, we target a different workload scenario emerging from a growing number of coarse-sound classification applications that require processing that can happen entirely cloud-free. For this distinctly different workload, we introduce general techniques that are applied at the level of the machine learning model, or the level of organization related to multiple algorithms for processing audio data. As such, the insights drawn from our work are directly applicable to a class of algorithms that build upon commonly adopted machine learning models in audio sensing.

Packet routing [31] and SSL encryption [37] leverage GPUs to increase processing throughput via batching of computations, but none of these works is focused on studying energy efficiency aspects which are critical for battery-powered devices.

GPU Resource Management. PTask [53] is an OS-level abstraction that attempts to introduce system-level guarantees such as fairness and performance isolation, since GPUs are not treated as a shared system resource and concurrent workloads interfere with each other. The relative difficulty in manually expressing algorithms in a data parallel manner may lead to missed optimization opportunities – works such as those of Zhang et al. [59] and Jog et al. [38] attempt to streamline the optimization process. The former improves GPU memory utilization and control flow by automatically removing data access irregularities, whereas the latter addresses problems with memory access latency at the thread scheduling level. Both types of optimizations are complementary to our work – we optimize the general structure of the parallel audio processing algorithms, while the mentioned frameworks tune parallel behavior of already built implementations. Last but not least, Sponge [35] provides a compiler framework that builds portable CUDA programs from a high-level streaming language. Instead, we study the trade-offs mobile GPUs provide for sensing, and build on top of OpenCL which together with the Qualcomm Adreno GPU dominates the mobile market.

9. CONCLUSION

In this paper we have studied the trade-offs of using a mobile GPU for audio sensing. We devised an optimization engine that leverages a set of structural and memory access parallel patterns to auto-tune GPU audio pipelines – optimized GPU routines are an order of magnitude faster than sequential CPU implementations, and up to 6.5x faster than cloud offloading (5Mbps throughput). With just 10-20 seconds of batched audio data, the optimized GPU begins to consume less energy than cloud offloading and in the range typical for low-power DSPs. The insights drawn can help towards the growth of the next-generation mobile sensing apps that leverage GPU capabilities for extreme runtime and energy performance.

10. ACKNOWLEDGMENTS

This work was supported by Microsoft Research through its PhD Scholarship Program. We thank the anonymous reviewers and our shepherd (Lin Zhong) for their valued comments and suggestions.

11. REFERENCES

- [1] Amazon Echo. <http://www.amazon.com/Amazon-Echo-Bluetooth-Speaker-with-WiFi-Alexa/dp/B00X4WHP5E>.
- [2] Apple Siri. <https://www.apple.com/uk/ios/siri/>.
- [3] GameBench. <https://www.gamebench.net/>.
- [4] Google Home. <https://home.google.com/>.
- [5] Google Now. <http://www.google.co.uk/landing/now/>.
- [6] HTK Speech Recognition Toolkit. <http://htk.eng.cam.ac.uk/>.
- [7] Intel Xeon Phi. <http://www.intel.com/content/www/us/en/processors/xeon/xeon-phi-detail.html>.
- [8] Monsoon Power Monitor. <http://www.msoon.com/LabEquipment/PowerMonitor/>.
- [9] NVIDIA CUDA. http://www.nvidia.com/object/cuda_home_new.html.
- [10] NVidia Tegra X1. <http://www.nvidia.com/object/tegra-x1-processor.html>.
- [11] OpenCL. <https://www.khronos.org/opencv/>.
- [12] Qualcomm Adreno GPU. <https://developer.qualcomm.com/software/adreno-gpu-sdk/gpu>.
- [13] Qualcomm Hexagon DSP. <https://developer.qualcomm.com/mobile-development/maximize-hardware/multimedia-optimization-hexagon-sdk/hexagon-dsp-processor>.
- [14] Qualcomm Hexagon SDK. <https://developer.qualcomm.com/mobile-development/maximize-hardware/multimedia-optimization-hexagon-sdk>.
- [15] Qualcomm Snapdragon 800 MDP. <http://goo.gl/ySfCfI>.
- [16] TensorFlow. <https://www.tensorflow.org/>.
- [17] Theano. <http://deeplearning.net/software/theano/>.
- [18] C. M. Bishop. *Pattern Recognition and Machine Learning (Information Science and Statistics)*. Springer-Verlag New York, Inc., Secaucus, NJ, USA, 2006.
- [19] S. Borkar and A. A. Chien. The future of microprocessors. *Commun. ACM*, 54(5):67–77, May 2011.
- [20] S. Campanoni, K. Brownell, S. Kanev, T. M. Jones, G.-Y. Wei, and D. Brooks. Helix-rc: An architecture-compiler co-design for automatic parallelization of irregular programs. In *Proceeding of the 41st Annual International Symposium on Computer Architecture*, ISCA '14, pages 217–228, Piscataway, NJ, USA, 2014. IEEE Press.
- [21] S. Campanoni, T. M. Jones, G. H. Holloway, G.-Y. Wei, and D. M. Brooks. Helix: Making the extraction of thread-level parallelism mainstream. *IEEE Micro*, 32(4):8–18, 2012.
- [22] G. Chen, C. Parada, and G. Heigold. Small-footprint keyword spotting using deep neural networks. In *IEEE International Conference on Acoustics, Speech, and Signal Processing*, ICASSP'14, 2014.
- [23] K. T. Cheng and Y. C. Wang. Using mobile gpu for general-purpose computing – a case study of face recognition on smartphones. In *VLSI Design, Automation and Test (VLSI-DAT)*, 2011 International Symposium on, pages 1–4, April 2011.
- [24] D. Chu, N. D. Lane, T. T.-T. Lai, C. Pang, X. Meng, Q. Guo, F. Li, and F. Zhao. Balancing energy, latency and accuracy for mobile sensor data classification. In *Proceedings of the 9th ACM Conference on Embedded Networked Sensor Systems*, SenSys '11, pages 54–67, New York, NY, USA, 2011. ACM.
- [25] A. de Cheveigné and H. Kawahara. YIN, a fundamental frequency estimator for speech and music. *The Journal of the Acoustical Society of America*, 111(4):1917–1930, 2002.
- [26] Z. Fang, Z. Guoliang, and S. Zhanjiang. Comparison of different implementations of mfcc. *J. Comput. Sci. Technol.*, 16(6):582–589, Nov. 2001.
- [27] P. Georgiev, N. D. Lane, K. K. Rachuri, and C. Mascolo. DSP.Ear: leveraging co-processor support for continuous audio sensing on smartphones. In *Proceedings of the 12th ACM Conference on Embedded Network Sensor Systems*, SenSys '14, New York, NY, USA, 2014. ACM.
- [28] P. Georgiev, N. D. Lane, K. K. Rachuri, and C. Mascolo. Leo: Scheduling sensor inference algorithms across heterogeneous mobile processors and network resources. In *Proceedings of the 22Nd Annual International Conference on Mobile Computing and Networking*, MobiCom '16, pages 320–333, New York, NY, USA, 2016. ACM.
- [29] K. Gupta and J. D. Owens. Compute & memory optimizations for high-quality speech recognition on low-end gpu processors. In *Proceedings of the 2011 18th International Conference on High Performance Computing*, HIPC '11, pages 1–10, Washington, DC, USA, 2011. IEEE Computer Society.
- [30] K. Han, D. Yu, and I. Tashev. Speech emotion recognition using deep neural network and extreme learning machine. In *Fifteenth Annual Conference of the International Speech Communication Association*, 2014.
- [31] S. Han, K. Jang, K. Park, and S. Moon. Packetshader: A gpu-accelerated software router. In *Proceedings of the ACM SIGCOMM 2010 Conference*, SIGCOMM '10, pages 195–206, New York, NY, USA, 2010. ACM.
- [32] H. Hermansky. Perceptual linear predictive (PLP) analysis of speech. *J. Acoust. Soc. Am.*, 57(4):1738–52, Apr. 1990.
- [33] G. Hinton, L. Deng, D. Yu, G. Dahl, A. rahman Mohamed, N. Jaitly, A. Senior, V. Vanhoucke, P. Nguyen, T. Sainath, and B. Kingsbury. Deep neural networks for acoustic modeling in speech recognition. *Signal Processing Magazine*, 2012.
- [34] G. Hinton, L. Deng, D. Yu, A. rahman Mohamed, N. Jaitly, A. Senior, V. Vanhoucke, P. Nguyen, T. S. G. Dahl, and B. Kingsbury. Deep neural networks for acoustic modeling in speech recognition. *IEEE Signal Processing Magazine*, 29(6):82–97, November 2012.
- [35] A. H. Hormati, M. Samadi, M. Woh, T. Mudge, and S. Mahlke. Sponge: Portable stream programming on graphics engines. In *Proceedings of the Sixteenth International Conference on Architectural Support for Programming Languages and Operating Systems*, ASPLOS XVI, pages 381–392, New York, NY, USA, 2011. ACM.
- [36] A. Huqqani, E. Schikuta, S. Yea, and P. Chena. Multicore and gpu parallelization of neural networks for face recognition. In *International Conference on Computational Science*, ICCS, Procedia Computer Science, pages 349–358, London, UK, June 2013. Elsevier.
- [37] K. Jang, S. Han, S. Han, S. Moon, and K. Park. Sslshader: Cheap ssl acceleration with commodity processors. In *Proceedings of the 8th USENIX Conference on Networked Systems Design and Implementation*, NSDI'11, pages 1–14, Berkeley, CA, USA, 2011. USENIX Association.

- [38] A. Jog, O. Kayiran, N. Chidambaram Nachiappan, A. K. Mishra, M. T. Kandemir, O. Mutlu, R. Iyer, and C. R. Das. Owl: Cooperative thread array aware scheduling techniques for improving gpgpu performance. In *Proceedings of the Eighteenth International Conference on Architectural Support for Programming Languages and Operating Systems, ASPLOS '13*, pages 395–406, New York, NY, USA, 2013. ACM.
- [39] D. B. Kirk and W.-m. W. Hwu. *Programming Massively Parallel Processors: A Hands-on Approach*. Morgan Kaufmann Publishers Inc., San Francisco, CA, USA, 1st edition, 2010.
- [40] N. D. Lane, S. Bhattacharya, P. Georgiev, C. Forlivesi, L. Jiao, L. Qendro, and F. Kawsar. Deepx: A software accelerator for low-power deep learning inference on mobile devices. In *2016 15th ACM/IEEE International Conference on Information Processing in Sensor Networks (IPSN)*, pages 1–12, April 2016.
- [41] N. D. Lane, S. Bhattacharya, P. Georgiev, C. Forlivesi, and F. Kawsar. An early resource characterization of deep learning on wearables, smartphones and internet-of-things devices. In *Proceedings of the 2015 International Workshop on Internet of Things Towards Applications, IoT-App '15*, pages 7–12, New York, NY, USA, 2015. ACM.
- [42] N. D. Lane, P. Georgiev, and L. Qendro. Deeppear: Robust smartphone audio sensing in unconstrained acoustic environments using deep learning. In *Proceedings of the 2015 ACM International Joint Conference on Pervasive and Ubiquitous Computing, UbiComp '15*, pages 283–294, New York, NY, USA, 2015. ACM.
- [43] Y. Lee, C. Min, C. Hwang, J. L. 0001, I. Hwang, Y. Ju, C. Yoo, M. Moon, U. Lee, and J. Song. Sociophone: everyday face-to-face interaction monitoring platform using multi-phone sensor fusion. In H.-H. Chu, P. Huang, R. R. Choudhury, and F. Zhao, editors, *MobiSys*, pages 499–500. ACM, 2013.
- [44] M. Liberman, K. Davis, M. Grossman, N. Martey, and J. Bell. Emotional prosody speech and transcripts. 2002.
- [45] H. Lu, A. J. B. Brush, B. Priyantha, A. K. Karlson, and J. Liu. Speakersense: Energy efficient unobtrusive speaker identification on mobile phones. In *Proceedings of the 9th International Conference on Pervasive Computing, Pervasive'11*, pages 188–205, Berlin, Heidelberg, 2011. Springer-Verlag.
- [46] H. Lu, D. Fraundorfer, M. Rabbi, M. S. Mast, G. T. Chittaranjan, A. T. Campbell, D. Gatica-Perez, and T. Choudhury. Stresssense: Detecting stress in unconstrained acoustic environments using smartphones. In *Proceedings of the 2012 ACM Conference on Ubiquitous Computing, UbiComp '12*, pages 351–360, New York, NY, USA, 2012. ACM.
- [47] H. Lu, J. Yang, Z. Liu, N. D. Lane, T. Choudhury, and A. T. Campbell. The jigsaw continuous sensing engine for mobile phone applications. In *Proceedings of the 8th ACM Conference on Embedded Networked Sensor Systems, SenSys '10*, pages 71–84, New York, NY, USA, 2010. ACM.
- [48] C. Luo and M. C. Chan. Socialweaver: Collaborative inference of human conversation networks using smartphones. In *Proceedings of the 11th ACM Conference on Embedded Networked Sensor Systems, SenSys '13*, pages 20:1–20:14, New York, NY, USA, 2013. ACM.
- [49] I. McLoughlin, H. Zhang, Z. Xie, Y. Song, and W. Xiao. Robust sound event classification using deep neural networks. *Trans. Audio, Speech and Lang. Proc.*, 23(3):540–552, Mar. 2015.
- [50] I. K. Park, N. Singhal, M. H. Lee, S. Cho, and C. Kim. Design and performance evaluation of image processing algorithms on gpus. *IEEE Trans. Parallel Distrib. Syst.*, 22(1):91–104, Jan. 2011.
- [51] B. Priyantha, D. Lymberopoulos, and J. Liu. Littlerock: Enabling energy-efficient continuous sensing on mobile phones. *IEEE Pervasive Computing*, 10(2):12–15, 2011.
- [52] K. K. Rachuri, M. Musolesi, C. Mascolo, P. J. Rentfrow, C. Longworth, and A. Aucinas. Emotionsense: A mobile phones based adaptive platform for experimental social psychology research. In *Proceedings of the 12th ACM International Conference on Ubiquitous Computing, Ubicomp '10*, pages 281–290, New York, NY, USA, 2010. ACM.
- [53] C. J. Rossbach, J. Currey, M. Silberstein, B. Ray, and E. Witchel. Ptask: Operating system abstractions to manage gpus as compute devices. In *Proceedings of the Twenty-Third ACM Symposium on Operating Systems Principles, SOSP '11*, pages 233–248, New York, NY, USA, 2011. ACM.
- [54] C. Shen, S. Chakraborty, K. R. Raghavan, H. Choi, and M. B. Srivastava. Exploiting processor heterogeneity for energy efficient context inference on mobile phones. In *Proceedings of the Workshop on Power-Aware Computing and Systems, HotPower '13*, pages 9:1–9:5, New York, NY, USA, 2013. ACM.
- [55] N. Singhal, I. K. Park, and S. Cho. Implementation and optimization of image processing algorithms on handheld gpu. In *Image Processing (ICIP), 2010 17th IEEE International Conference on*, pages 4481–4484, Sept 2010.
- [56] S. Verma, A. Robinson, and P. Dutta. Audiodaq: Turning the mobile phone's ubiquitous headset port into a universal data acquisition interface. In *Proceedings of the 10th ACM Conference on Embedded Network Sensor Systems, SenSys '12*, pages 197–210, New York, NY, USA, 2012. ACM.
- [57] G. Wang, Y. Xiong, J. Yun, and J. R. Cavallaro. Accelerating computer vision algorithms using opencv framework on the mobile gpu - a case study. In *ICASSP*, pages 2629–2633. IEEE, 2013.
- [58] C. Xu, S. Li, G. Liu, Y. Zhang, E. Miluzzo, Y.-F. Chen, J. Li, and B. Finer. Crowd++: Unsupervised speaker count with smartphones. In *Proceedings of the 2013 ACM International Joint Conference on Pervasive and Ubiquitous Computing, UbiComp '13*, pages 43–52, New York, NY, USA, 2013. ACM.
- [59] E. Z. Zhang, Y. Jiang, Z. Guo, K. Tian, and X. Shen. On-the-fly elimination of dynamic irregularities for gpu computing. In *Proceedings of the Sixteenth International Conference on Architectural Support for Programming Languages and Operating Systems, ASPLOS XVI*, pages 369–380, New York, NY, USA, 2011. ACM.
- [60] Y. Zhang, K. Adl, and J. Glass. Fast spoken query detection using lower-bound dynamic time warping on graphical processing units. In *In Proc. ICASSP*, pages 5173–5176, 2012.
- [61] G. Zhou, J. H. L. Hansen, and J. F. Kaiser. Nonlinear feature based classification of speech under stress. *IEEE Transactions on Speech and Audio Processing*, 9(3):201–216, 2001.